HHS Public Access

Author manuscript

J Comp Neurol. Author manuscript; available in PMC 2024 October 01.

Published in final edited form as:

J Comp Neurol. 2023 October ; 531(15): 1550–1561. doi:10.1002/cne.25528.

Loss of TRPC2 Function in Mice Alters Sex Differences in Brain Regions Regulating Social Behaviors

D.R. Pfau,

S. Baribeau,

F. Brown,

N. Khetarpal,

S.M. Breedlove,

C.L. Jordan

Neuroscience Program, Michigan State University, East Lansing, Michigan

Abstract

The transient receptor potential cation channel 2 (TRPC2) conveys pheromonal information from the vomeronasal organ (VNO) to the brain. Both male and female mice lacking this gene show altered sex-typical behavior as adults. We asked whether TRPC2, highly expressed in the vomeronasal organ (VNO), normally participates in the development of VNO-recipient brain regions controlling mounting and aggression, two behaviors affected by TRPC2 loss. We now report significant effects of TRPC2 loss in both the posterodorsal aspect of the medial amygdala (MePD) and ventromedial nucleus of the hypothalamus (VMN) of male and female mice. In the MePD, a sex difference in neuron number was eliminated by the TRPC2 knockout (KO), but the effect was complex, with fewer neurons in the *right* MePD of females, and fewer neurons in the *left* MePD of males. In contrast, MePD astrocytes were unaffected by the KO. In the ventrolateral (vl) aspect of the VMH, KO females were like wildtype (WT) females but TRPC2 loss had a dramatic effect in males, with fewer neurons than WT males and a smaller VMHvl overall. We also discovered a glial sex difference in VMHvl of WTs, with females having more astrocytes than males. Interestingly, TRPC2 loss *increased* astrocyte number in males in this region. We conclude that TRPC2 normally participates in sexual differentiation of the mouse MePD and VMHvl. These changes in two key VNO-recipient regions may underlie the effects of the TRPC2 KO on behavior.

Loss of a functional *TRPC2* gene alters anatomical sex differences in the posterodorsal medial amygdala and ventromedial hypothalamic nucleus ventrolateral subdivision of adult mice. *TRPC2*

*Corresponding Author: Daniel Pfau, Michigan State University, Neuroscience Program, 293 Farm Lane, East Lansing, MI 48824, Pfaud@umich.edu.

*Obstetrics & Gynecology, University of Michigan, 1101 Beal Ave, Lurie Biomedical Engineering Building, Ann Arbor, MI 48109

**Department of Psychology, Michigan State University, East Lansing, MI

Author rolls: All authors had full access to all the data in the study and take responsibility for the integrity of the data and the accuracy of the data analysis. Study concept and design: DRP, CLJ, SMB. Acquisition of data: DRP, SB, NK, FB. Analysis and interpretation of data: DRP, FB, CLJ. Drafting of the manuscript: DRP, CLJ. Critical revision of the manuscript for important intellectual content: DRP, CLJ, SMB. Statistical analysis: DRP, CLJ. Obtained funding: CLJ, SMB. Administrative, technical, and material support: CLJ, SB, NK, FB. Study supervision: CLJ

Conflict of interest: The authors claim no conflict of interest.

presence influenced the unique male and female anatomy of the amygdala while the impact on the hypothalamus was largely limited to males.

Graphical Abstract

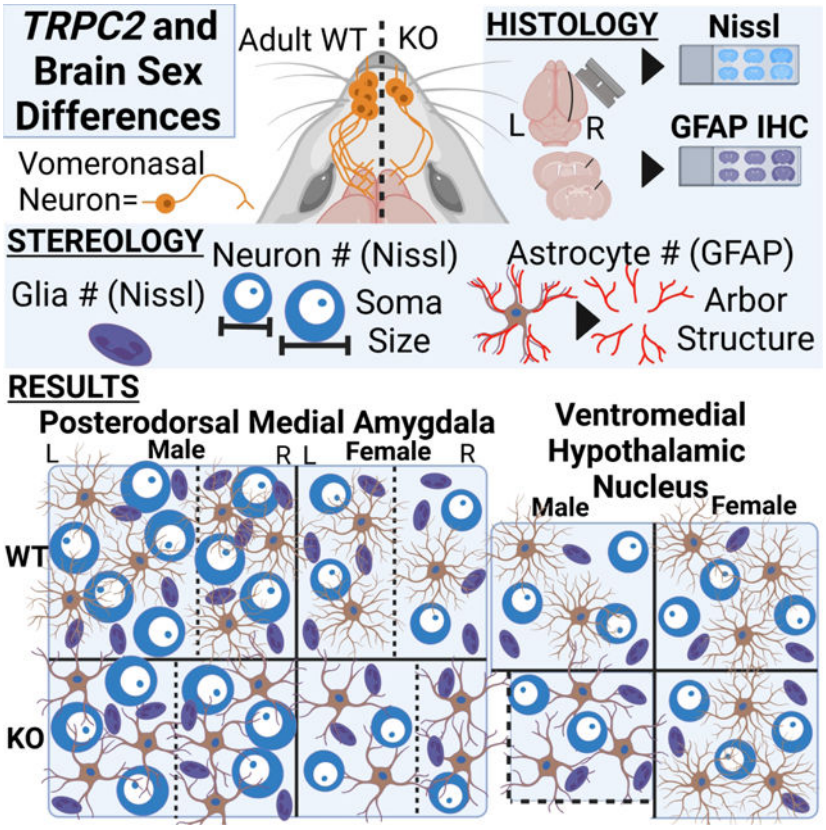

Keywords

amygdala; hypothalamus; astrocyte; sex difference; laterality; neuron; stereology

Introduction

Considerable evidence indicates that sex differences in gonadal hormones drive sex differences in brain and behavior (1, 2). Recent work supports the idea that brain sexual differentiation is also regulated by signals from the periphery (3). One such peripheral influence is the accessory olfactory system, starting with sensory information from the vomeronasal organ (VNO). After a VNO neuron detects pheromones in the environment, the transient receptor potential cation channel 2 (TRPC2) transduces the chemical signal into action potentials that are sent to the accessory olfactory bulb (AOB) (4). Sex differences in the expression of vomeronasal receptors, could allow the same environment to uniquely activate the male and female VNO (5). Ultimately, this information is processed in the amygdala and hypothalamus (6), two regions that are sexually differentiated (7–9) and facilitate sex-specific sexual and aggressive behaviors (2, 10, 11). Notably, these same

behaviors are altered in mice without a functional TRPC2 gene (KO) (12, 13), raising the question of whether TRPC2 also normally participates in the formation of morphological sex differences in these same brain areas.

The expression of sex-specific behaviors depends on a functional VNO and sex-specific pheromones. For example, the expression of a mounting preference in naïve male rodents depends on receiving female-specific and VNO-dependent pheromonal signals (14, 15). As naïve WT males express sexual behaviors towards receptive females, limbic neuron activity changes across appetitive and consummatory events. The neuronal activity seen in WT males during their initial olfactory investigations is absent in TRPC2 KO males (16) and they lack a preference in sexual partners, mounting *both* males and females (13). Perhaps more striking is the robust and frequent expression of mounting behavior in TRPC2 KO females, a behavior that typically requires testosterone treatment (17). Like KO males, KO females will mount *both* male and female mice (18). Several other behaviors known to involve pheromones in rodents are altered as well. TRPC2 loss eliminates maternal aggression in females (19) and male-directed aggression in males (13). In short, pheromone-dependent behaviors that are sex-specific are selectively altered in TRPC2 KO mice. Importantly, these same behaviors do not appear following VNO ablation in adulthood (14, 17). However, the effect of the TRPC2 KO is life-long, which could affect the development of relevant brain regions.

The neural basis for these changes in social behavior is largely unknown, with only a few studies showing anatomical changes in relevant brain regions. For example, while the number of projections from the VNO to AOB is initially normal in TRPC2 KO mice, a deficit emerges as development proceeds (13). Adult KO mice also have fewer mature sensory neurons in the VNO compared with WTs . These two factors undoubtedly reduce the transmission of pheromonal information to downstream brain regions. Indeed, KO mice have a smaller AOB and, importantly, the effects of the TRPC2 KO on the AOB vary by sex (19). Sex differences in these sensory neurons or their function may be critical for the appearance of sex differences in the central nervous system, a possibility we examine here.

Sex-typical behaviors like mounting and aggression involve several nuclei along the VNO-recipient pathway that also show sex differences, but do not express TRPC2 (20), notably, the posterodorsal aspect of the medial amygdala (MePD) (8, 21) and ventromedial nucleus of the hypothalamus (VMH) (2). The MePD mediates courtship/copulatory behavior in mice (21–23) and has sex differences in volume, neuron number, neuron soma size, and astrocyte number in mice (8) and/or rats (24–26). Importantly, several sex differences in the rodent MePD also vary by hemisphere (8, 26). The ventrolateral subdivision of the VMH (VMHvl) has sex differences (2, 9, 27) and contains neurons critical for the expression of male mounting and aggression (11) and female sexual behavior (2). We characterized the morphology of the MePD and VMHvl in KO and WT mice of both sexes using Nissl staining and immunostaining for glial fibrillary acidic protein (GFAP), yielding measures of regional volume, and number of neurons, total glia, and astrocytes. Given cell number may be permanently organized by adulthood, we also assessed aspects of cell morphology within each region. We find that the effect of TRPC2 KO on these brain regions is complex, with sex differences in morphology sometimes eliminated and sometimes introduced by virtue of

the KO. KO mice show overall deficits in the number of cells in the MePD and VMHvl, although the extent of these deficits depends on sex and/or hemisphere. Such morphological changes initiated by the loss of TRPC2 function likely contribute to the unique behavioral outcomes observed in KO mice.

Materials and methods

Animals:

TRPC2 KO (B6;129S1-Trpc2tm1Dlc/J JAX stock number: 021208) mice and WT mice (B6129SF2/J021208; JAX stock number: 101045) were purchased and used to establish homozygous TRPC2 KO and WT breeding pairs, respectively. F1 pups from these homozygous pairings were weaned at postnatal day (PD) 21, ear punched, housed with same-sex littermates and remained unmanipulated until tissue collection. Adult (PD 84–105) age-matched WT and KO mice were overdosed with sodium pentobarbital (210 mg/kg) and perfused transcardially with 0.9% saline followed by phosphate buffered (0.1M, pH 7.4) 4% paraformaldehyde. Male and female mice were categorized based on external markers and testicle presence, PCR for *SRY* confirmed categorizations (28). Brains were harvested and postfixed 2 hours in the same paraformaldehyde solution (room temperature) followed by cryoprotection in 20% sucrose in 0.1M phosphate buffer for at least 48 hours at 4° C. Brains were scored along the right dorsal surface of the cortex to mark side and then cross sectioned at 30 microns on a freezing sliding microtome. Three adjacent series were collected and stored at −20°C in de Olmos cryoprotectant (29) until stained. All animal procedures were approved by the Institutional Animal Care and Use Committee at Michigan State University.

Nissl staining:

One series of sections was brought to room temperature, rinsed, and mounted onto gel-subbed slides. Once dry and defatted, sections were stained with thionin (8), dehydrated, cleared, and coverslipped with Permount (Fisher Scientific). This protocol results in distinct staining characteristics for neurons and glia, allowing for counts of each. Neurons were identified based on presence of a cytoplasmic shell surrounding a distinct nucleus and nucleolus. Glial cells, which included astrocytes, were identified based on the absence of an apparent cytoplasmic compartment but with a distinct nucleus often containing lobed nucleoli.

Glial fibrillary acidic protein immunohistological staining:

The second series was brought to room temperature and rinsed with phosphate buffered saline (0.1M, pH 7.4) containing 0.3% Triton and 0.1% gelatin (PBS-GT). This same solution was used throughout as the vehicle for immunoreagents and rinses. Following a published protocol for GFAP immunostaining of astrocytes in mice (8), sections were incubated in 0.5% sodium borohydride in PBS-GT (15 min) and blocked for nonspecific avidin-biotin binding (Avidin and Biotin blocking kit, SP-2001, Vector, Burlingame, CA), followed by an overnight incubation at 4°C in monoclonal mouse anti-GFAP (EMD Millipore Cat# MAB360, RRID:AB_2109815, 1:50,000 dilution). Sections were then incubated in biotinylated horse anti-mouse secondary antibody (Vector Laboratories Cat# BA-2001, RRID:AB_2336180, 1:2,500 dilution) followed by incubation in half-

strength peroxidase avidin-biotin complex solution (Elite Avidin Biotin complex kit, PK-6100, Vector Laboratories, Burlingame, CA) and reacted for 5 minutes using 0.025% diaminobenzidine (DAB, Sigma, St. Louis, MO) with 0.0125% H2O2 in Tris buffer (0.05M, pH 7.2), to visualize horseradish peroxidase. After rinsing to quench the reaction, sections were mounted onto gel-subbed slides and allowed to dry before counterstaining with Harris's Hematoxylin solution (Sigma, #010M4354), followed by alcohol dehydration, clearing, and coverslipping with Permount.

Antibody characterization:

A full list of antibodies used can be found in Table 1. As has been previously reported in our lab, staining was absent when the primary antiserum was omitted and reliably led to the visualization of morphology resembling that of astrocytes (8).

Stereological analysis:

Stereological analysis was performed on a Zeiss Axioplan II microscope equipped with an Optronics MicroFire digital video camera and StereoInvestigator software (v. 7.0, MBF Bioscience, Williston, VT). The total numbers of neurons, glia, and astrocytes were determined throughout the rostrocaudal extent of the MePD, and the ventrolateral (vl) subregion of the VMH, while neurons and glia, but not astrocytes were counted in the dorsomedial (dm) subdivision. At low magnification, regional boundaries were traced in each section. Regions were identified based on a mouse atlas (30) and previously published representative images and parameters for the MePD of C57Bl/6J mice (8). To outline the MePD (Bregma −1.34mm to −2.06 mm), landmarks visible in both Nissl and hematoxylin-stained sections included the optic tract, shape of the stria terminalis and posteroventral medial amygdala. Parameters used to identify the VMH of rats were modified to examine mice (27). The arcuate nucleus and third ventricle acted as the main landmarks for the VMH in Nissl (see results) and hematoxylin-stained sections.

Neurons and glia were counted in Nissl-stained sections using a 100X Zeiss plan-neofluar oil-immersion objective (na=1.3). Previously defined characteristics and images were used to identify neuron and glia (8). Slides were coded, making the observer blind to the sex and genotype of the animal. The optical fractionator probe was used to produce unbiased counts of the number of neurons and overall glial cells in Nissl-stained sections. To measure the size of neuronal soma, the perimeter of neurons from five randomly selected contours were traced. The StereoInvestigator optical fractionator setup was used to pick five random sites within each of the five contours, with a total of 25 cells traced per hemisphere. The neuronal soma closest to the optical fractionator probe was traced using the nucleator probe and 100X objective. Astrocytes were counted using the optical fractionator probe in GFAP-labeled sections with a 40X Zeiss plan-neofluar objective (na = 0.75). Astrocytes were identified and counted based on having three or more GFAP-labeled fibers surrounding a distinct hematoxylin-stained nucleus.

These methods provided estimates of the total number of neurons, overall glial cells, and astrocytes, along with regional volumes and neuronal soma size. If one section was missing, the average cell number of adjacent sections was included in the program's estimation, but

if more than one section was damaged or missing, the brain was excluded from the analysis. The program does not permit users to include averaged regional areas in its estimations, accounting for the lower sample sizes reported for volume measures.

Neurolucida software (v. 7.0, MBF Bioscience) was used to trace and estimate the complexity of astrocyte arbors. In five randomly selected MePD and VMHvl regions from each animal, the entire GFAP-stained arbor of two astrocytes randomly selected by an observer blind to sex and genotype were traced using the 100X objective, with ten astrocytes sampled from the MePD of each hemisphere. Based on these traces, the average number of primary processes, average number of branch points, average number of branch endings, total length and average branch length were calculated for each animal and hemisphere.

Statistical analysis:

Separate ANOVAs were used to examine each measure (regional volume, neuron number, overall glial number, neuron soma size, astrocyte number and process complexity) within each brain region. For the MePD and the VMH regions, a 3-way mixed design ANOVA was utilized, with laterality as the within-subjects variable, and sex and genotype as between-subject variables. This was followed by conservative posthoc Bonferroni comparisons to examine significant main effects and interactions. Results reported are means ± standard errors of the mean (SEM) with alpha set at 0.05.

Results

Posterodorsal aspect of the medial amygdala:

Regional volume: MePD volume in Nissl-stained sections depended on both genotype ($F_{(1,25)}$=8.84, p=0.006, d=1.06) and sex ($F_{(1,25)}$=19.7, p<0.001, d=1.58; Figure 1). Total MePD volume, the sum of both hemispheres, is larger in WT mice (44.4 $mm^3 \times 10^{-2}$ ± 1.7) than KO mice (37.2 $mm^3 \times 10^{-2}$ ± 1.8) and larger in males (46.2 $mm^3 \times 10^2$ ± 1.7) than females (35.4 $mm^3 \times 10^{-2}$ ±1.8). There was also a main effect of laterality, with the left MePD larger than the right ($F_{(1,25)}$=3.65, p=0.019, d=0.44) and a three-way interaction between hemisphere, sex and genotype ($F_{(1,25)}$=11.6, p=0.01). Posthoc analyses indicated that volume of the MePD is sexually differentiated in WTs on both the left (p<0.001, d=2.03) and right hemisphere (p=0.035, d=1.24), whereas TRPC2 KO mice had a sex difference only on the right (p=0.002, d=1.83) and not the left hemisphere (p=0.11). Moreover, MePD volume was reduced in TRPC2 KO mice in both a sex– and side-specific manner, with the right MePD smaller in KO females than WT females (p=0.049, d=1.15), and the left MePD smaller in KO males than WT males (p=0.002, d=0.95). Knocking out the TRPC2 gene also affected which sex was lateralized in MePD volume; the left-bias seen in WT males (p=0.008, d=1.2; Figure 1) was lost in KO males (p=0.45), but gained in KO females (p=0.028, d=2.1). In sum, deletion of TRPC2 reduced both the volume of the MePD and its sex differences.

Neuron number and soma size: Cell counts of MePD neurons in Nissl-stained slices revealed a significant effect of sex ($F_{(1,29)}$=8.24, p=0.008, d=0.99), with males having more neurons overall than females regardless of whether TRPC2 was functional (Figure 2A).

There was also a main effect of laterality ($F_{(1,29)}$=7.44, p=0.011, d=0.29) with the left MePD containing more neurons overall than the right. While there was only a marginal effect of genotype on MePD neuron number ($F_{(1,29)}$=3.16, p=0.086), there was a three-way interaction of sex, genotype and hemisphere ($F_{(1,29)}$=12.47, p=0.001). Further analyses revealed a sex difference in MePD neuron number only on the left of WT mice (p=0.011, d=1.34), and only on the right of KO mice (p=0.014, d=1.38). Moreover, neuron number was reduced on the right of KO females compared to WT females (p=0.046, d=1.03), and on the left of KO males compared to WT males (p=0.041, d=0.93). As a result of these lateralized effects of the TRPC2 KO on MePD neuron number, KO females have significantly more neurons in the left MePD than the right (p=0.001, d=0.79; Figure 2A), similar to WT males (p=0.02, d=0.52), whereas KO males, like WT females, exhibit no laterality in MePD neuron number (WT female p=0.59, KO males p=0.8). There was also an overall sex difference in the size of neuronal somata in the MePD, with neurons being larger in males than in females ($F_{(1,25)}$=12.62, p=0.002, d=1.67; Figure 2B.i). The size of neuronal somata in the MePD was independent of both the TRPC2 gene ($F_{(1,25)}$=0.1, p=0.754) and hemisphere ($F_{(1,25)}$=2.55, p=0.12) with no interactions between these variable and sex (Figure 2B).

Glia Number: Counts of all glial cells in Nissl-stained MePD revealed main effects of both sex and genotype; males had more glia than females ($F_{(1,29)}$=7.86, p=0.009, d=1.21) and KO mice had fewer glia than WT mice ($F_{(1,29)}$=11.59, p=0.002, d=1; Figure 2C). There was also an overall effect of hemisphere with more glia present in the left compared to the right hemisphere ($F_{(1,29)}$=8.7, p=0.006, d=1.6). No interactions were significant for this measure.

Astrocyte number and branch complexity: Like our counts of glia in Nissl-stained sections, counts of astrocytes visualized by GFAP in the MePD showed an overall sex difference, with males having more MePD astrocytes than females ($F_{(1,26)}$=16.44, p>0.0001, d=1.17; Figure 2D), similar to previous findings (8). However, unlike overall glial cell number, TRPC2 KO had no effect on the number of MePD astrocytes ($F_{(1,26)}$=0.299, p=0.59), suggesting TRPC2 regulates glial cells other than astrocytes to account for effects of overall glial numbers in Nissl stain. While no overall effects of laterality were found ($F_{(1,26)}$=3.85, p=0.06), sex interacted with hemisphere ($F_{(1,26)}$=6.17, p=0.02), as both KO and WT females had more astrocytes on the left than right (p=0.004, d=0.49; Figure 2D).

The complexity of MePD astrocytes was unaffected by sex, laterality and genotype (Table 2) with one exception; KO mice have fewer branch endings than WTs ($F_{(1,16)}$=4.48, p=0.05, d=0.9). Given the number of independent F tests on related parameters from the same data, this may be a type I error despite the large effect size.

In sum, the MePD displays robust sex differences in most cellular and volumetric measures in WT mice. The effect of knocking out TRPC2 on these sex differences are complex, with sex differences conserved, absent, minimized, or introduced depending on the cellular parameter being measured. Moreover, a continuing theme of the MePD is its marked laterality, which is also susceptible to the influence of TRPC2, with its effects comparably complex.

Ventromedial Nucleus of the hypothalamus:

Regional volume: Dense cell populations with a cell-poor central region between them and surrounded by a capsule formed the VMHdm and VMHvl (Figure 3A, B; bregma −1.31mm to −2.03mm). Both regions were identifiable throughout the medial hypothalamus due to the lower cell densities of the surrounding tissue. In Nissl-stained VMH, neither sex ($F_{(1,19)}$=2.7, p=0.12), nor genotype ($F_{(1,19)}$=2.69, p=0.12), nor hemisphere ($F_{(1,19)}$=0.99, p=0.33) significantly influenced the volume of the VMHvl. In contrast to the MePD, we found no evidence of laterality in any measure of the VMH.

However, there were marginally significant interactions between sex and genotype on VMHvl volume ($F_{(1,19)}$=4.3, p=0.052), prompting posthoc Bonferroni analyses. While VMHvl volume was equal in WT males and females (p=0.36), it was smaller in males than females in the KO mice (p=0.017, d=1; Figure 3C). WT males also had larger VMHvl than KO males (p=0.013; d=0.8). The loss of VMHvl volume in KO males introduces a sex difference in KOs that is absent in WT mice. In contrast, we found no differences in the volume of the VMHdm based on Nissl staining (Figure 3D).

Neuron number and soma size: The number of neurons in the VMHvl varied by both sex ($F_{(1,25)}$=6.88, p=0.015) and genotype ($F_{(1,25)}$=7.39, p=0.012; Figure 4A) but not hemisphere ($F_{(1,25)}$=0.053, p=0.82). A significant interaction between sex and genotype was also found ($F_{(1,25)}$=7.57, p=0.011). Posthoc analyses indicated that while WT mice showed no sex difference (p=0.927) in neuron number, KO mice did (Figure 4A). In KO mice, males had fewer neurons than females (p=0.001, d=1.86), aligning with the effect of the KO on VMHvl volume. KO males also had significantly fewer neurons than WT males (p<0.001, d=1.9). Overall, the size of VMHvl neuronal somata were similar between the sexes ($F_{(1,25)}$=1.2, p=0.28) and across hemispheres ($F_{(1,25)}$=1.5, p=0.3), but WT mice had larger neuronal somata than KOs ($F_{(1,25)}$=4.28, p=0.049, d=2; Figure 4B), indicating a main effect of genotype but not sex. These two factors did not interact ($F_{(1,25)}$=0.96, p=0.34). In sum, TRPC2 KO reduced the size of neurons in the VMHvl of males and females and reduced the regional volume and number of neurons in males only.

Glia number: We found no significant effects of sex, genotype, or laterality on glial cell number in Nissl-stained VMHvl (Figure 4C).

Astrocyte number and branch complexity: The number of astrocytes in the VMHvl revealed no overall effect of sex ($F_{(1,30)}$=1.31, p=0.26), nor genotype ($F_{(1,30)}$=3.36, p=0.08), nor hemisphere ($F_{(1,30)}$=0.71, p=0.41). There was however a significant interaction between sex and genotype ($F_{(1,30)}$=10.34, p=003; Figure 4D). In WT mice, females had more VMHvl astrocytes than males (p=0.004, d=1.6), a sex difference that is absent in KO mice (p=0.162), caused by a selective increase in astrocytes in KO males compared to WT males (p=0.002, d=1.8). Notably, this is the only variable that is increased by TRPC2 loss.

Some measures of astrocyte complexity in the VMHvl were affected by the TRPC2 KO (Table 3). KO mice had fewer nodes ($F_{(1,17)}$=8.04, p=0.012, d=1.15) but this effect depended on sex ($F_{(1,17)}$=4.47, p=0.05). Posthoc analysis revealed no sex difference in WTs (p=0.554) but a sex difference in KOs, with VMHvl astrocytes of KO males having fewer nodes

than those of KO females (p=0.027, d=1.4). VMHvl astrocytes in males also had fewer nodes in KO mice than WTs (p=0.002, d=2). The number of branch endings showed an overall sex difference ($F_{(1,17)}$=5.68, p=0.029, d=1.1) and this main effect also depended on genotype ($F_{(1,17)}$=4.65, p=0.046), with KO males having fewer branch endings than both KO females (p=0.004, d=2.1) and WT males (p=0.017, d=2). These data suggest that astrocytes in the VMHvl are notably simpler in KO males, which could affect the degree of synaptic connectivity carrying behaviorally relevant signals. Finally, there was a significant interaction between sex, genotype and hemisphere on branch length ($F_{(1,17)}$=6.8, p=0.019) without significant main effects of these variables separately. Posthoc analysis indicated that astrocyte branch length in the VMHvl of WT females was lateralized, with longer branches appearing in the right hemisphere (Table 3). This was the only effect of hemisphere found in the VMHvl and could be a type I error.

In contrast to measures of the vl portion of the VMH, we found no effects of either sex or genotype in the dm subdivision (Figure 4E, 4F).

In sum, the VMHvl of WT mice displays few sex differences in overall morphology and virtually no laterality. The role of TRPC2 in the neuroanatomical development of the VMHvl appears specific to males, resulting in several sex differences in KO mice not seen in WT mice.

Discussion

Sex differences in brain circuitry are presumed critical for the expression of sex-typical behaviors (2, 31), including aggression and sex behavior. Because these behaviors are affected in TRPC2 null mice (12), we asked whether the cellular attributes of two forebrain regions, the posterodorsal aspect of the medial amygdala (MePD) and ventromedial nucleus of the hypothalamus ventrolateral subdivision (VMHvl), implicated in the control of these behaviors were also affected. We now report that both the MePD and VMHvl are indeed altered in TRPC2 KO mice, with the effects of the KO greater in the MePD than the VMHvl. For some measures, sex differences in WT mice were lost in the KO mice while, for other measures, new sex differences were gained. Such changes in TRPC2 null mice suggest that TRPC2-dependent processes guide sexual differentiation of mouse brain nuclei, influencing sex-specific aggressive and sexual behavior. Our findings also show for the first time that the MePD in WT mice is both sexually differentiated and lateralized, as had been reported for C57Bl/6J mice (8), and for rats (24, 26, 32). The VMHvl, also not previously characterized in WT mice, has sex differences in several parameters, but is not lateralized, aligning well with findings from rats (9).

TRPC2 loss alters the male and female MePD:

In WT mice, the MePD is larger overall (Figure 1) with more neurons, glia and astrocytes, and larger neuronal soma in males than females (Figure 2), aligning with findings from other mouse strains. For example, males of three different strains (BALB/c, C57Bl/6J and B6129S; Figures 1, 2) have a larger MePD with larger neuronal somata than females (8, 33). Current data also align with previous reports of a sex difference with males having a greater number of neurons and astrocytes in C57Bl/6J mice, with a comparably marked laterality

in these measures (8). Thus, the constancy of sex differences and laterality in MePD cell number and/or size across three different mouse strains suggest that these cellular attributes may critically mediate the expression of sex differences in sexual behavior preserved across strains.

Notably, several measures in the MePD were altered in TRPC2 KO mice, showing decreases in regional volume, and in the number of neurons, glia, and astrocytic arbor complexity. The effects on regional volume eliminated laterality in KO males and induced laterality in KO females (Figure 1). Perhaps one reason KO females exhibit male-like sex behavior is because they have acquired this masculinized lateralization of MePD volume. For both WT males and KO females, the left MePD is larger than the right. These shifts in volume are also accompanied by similar changes in MePD neuron number, with KO females having lateralized neuron numbers, in the same manner as WT males (Figure 2Bii). Other effects of the KO on MePD morphology include fewer total glia (Figure 2), and astrocytic fiber endings (Table 2). These data support the idea that sexual differentiation of the MePD depends on TRPC2 and may underlie the effects of TRPC2 KO on behavior in males and females.

There is considerable evidence that the MePD plays a role in sexual and aggressive behaviors. For example, in males, loss of the MePD affects sexual behaviors (34), including an odor preference for urine from the opposite sex, a critical component in directing sex behavior of males toward females (7, 35). Losses in MePD volume and cell number in KO males may contribute to their loss of an odor preference (13). However, this idea raises the question of *which* MePD neurons might be lacking in TRPC2 KO mice. The preference for urine from the opposite sex in males may depend on specific subpopulations of MePD projection neurons. For example, disconnecting the MePD from the extended medial amygdala disrupts this preference in hamsters (35), similar to what is seen in KO male mice (13). Staining specific neuronal subtypes would provide information necessary to determine whether changes in the TRPC2 KO mouse brain may influence behavior.

Whether MePD neurons are lost in the right or left hemisphere may also be important. The rodent brain shows lateralized responses while processing olfactory cues (37, 38) and most VNO signals remain ipsilateral (39). Male mice preferentially examine novel female scents with the *right* nostril (40) while familiar scent detection occurs through the *left* nostril in dogs (41). The organization and activation of a female-urine odor preference in males requires detection of both a novel and familiar scent which, if processed by the MePD, may occur within the *right* and *left* hemispheres respectively. That lateralized function may contribute to the changes in behavior of KO mice underscores the importance of tracking morphological and functional changes in each hemisphere of the MePD.

TRPC2 KO female mice are particularly interesting in their apparent loss of mate recognition and maternal aggression. Notably, the MePD has been implicated in the control of both of those behaviors (23). Estrous females find novel male pheromones attractive (42, 43) while lactating dams will respond aggressively towards an animal carrying a novel male scent (14). The loss of maternal aggression in lactating TRPC2 KO dams (19) is associated with a reduced c-fos response to novel male urine in their MePD compared

with WT females (44). While MePD laterality was not examined in those studies, c-fos increases in the right AOB of WT females exposed to a novel male intruder but not in KOs (19). Interestingly, we find a deficit in the number of neurons only in the *right* MePD of KO females compared to WT females (Figure 2Aii). Because in mammals the right nostril is tied to detecting unfamiliar scents (45, 46), perhaps those neurons lost in the right MePD of KO females are involved in the expression of maternal aggression. However, the picture is not a simple one, since KO females retain the "Bruce Effect" and are able to abort pre-implanted embryos when exposed to a novel male scent (47). While these findings appear contradictory, the outcomes represent different domains of pheromone responses. Blocking pregnancy by delaying implantation involves a physiological response (48) while maternal aggression is a behavioral response (49). The circuits influencing pheromone-induced behavior or hormone release are distinct (50, 51). These data further support the importance of identifying which MePD neuronal populations are affected after TRPC2 KO.

While neurons are often considered the active components of the nervous system, glia play a dynamic role in brain function (57) and may contribute to brain sex differences (58). When examining the total glial cell population in adult WT mice, we found a sex difference absent in C57Bl/6J mice (Figure 2Ci) (8). This sex difference may extend to multiple glial subtypes, i.e. microglia, astrocytes, oligodendrocytes. We know astrocytes contribute to an overall glial sex difference (Figure 2Di) but the sex difference in glial number exceeds that of astrocytes (Figure 2Ci). We also know that, along with astrocytes, microglia respond to steroid hormones to support the production of sex differences in other brain measures (59–61) and sex differences in the glial population itself may facilitate this process (62). The sex difference in WTs likely involves multiple glia subtypes and sources, as both circulating steroid hormone milieus and sex chromosome complement may drive glia-dependent sex differences (58). Since astrocyte number is independent of genotype, glial loss in KOs appears outside the astrocyte population. Critical targets for future MePD research in TRPC2 mice include both neuronal and glial characteristics.

TRPC2 loss alters the male VMHvl:

Male rats have a larger VMHvl than females (63), accompanied by larger neuronal somata (9), greater neuropil volume (27), more extensive dendritic arbors (64), and more afferent fibers from the fornix (65). In rats, both high circulating testosterone and androgen receptors are necessary for the sex differences in VMHvl volume (9, 63). Compared with the rat, relatively little is known regarding the anatomy and steroid responsiveness of the mouse VMHvl. Here, we find no sex differences in VMHvl volume (Figure 3A) neuronal number (Figure 4A), nor neuron soma size (Figure 4B). We find WT female mice have more astrocytes than males in the VMHvl (Figure 4D) and the GFAP-ir fibers in females have more endings (Table 3). This sex difference may be influenced by gonadal hormones as male mice lacking the androgen receptor show an increase in hypothalamic astrocytes (66). Compared to the MePD, the VMHvl of WT mice has little laterality and few overall sex differences. Still, several VMHvl measures were influenced by TRPC2 loss.

Overall, KO mice have smaller neurons than WTs (Figure 4C) while other effects of genotype depended on sex. We found KO males have a smaller VMHvl (Figure 3A) with fewer neurons (Figure 4A) compared with WT males. Neurons in the male VMHvl are critical for social behavior (11, 67). In males, the same neurons expressing estrogen receptor-alpha (Esr1) exert control over sexual and aggressive behaviors. When these Esr1+ neurons are weakly activated, males mount intruders (11). Increasing Esr1+ neuron activation or activating the entire VMHvl generates attack behavior (11, 67). TRPC2 function may influence Esr1+ neurons as KO males are capable of mounting but not aggression (12). Because knocking out ER entirely within the VMH greatly reduces male sexual behaviors (68), the Esr1+ neuron population in KOs must be sufficient to induce mounting but incapable of reaching the activation required for seeking aggression. Male KOs have more VMHvl astrocytes than WT males, eliminating the sex difference seen in WTs (Figure 4D). Despite having more VMHvl astrocytes, the GFAP-ir fibers of KO males have fewer nodes and endings than any other group (Table 3). Astrocytes are known to contribute to cellular signaling (69) and assist in the scalable activation of another hypothalamic region (70). Astrocytes may play a similar role in VMHvl activation. Therefore, in addition to neuronal changes, the increased number of VMHvl astrocytes or decreased arbor complexity in KO males may relate to changes in their aggression and mounting.

We found relatively few structural changes to the female VMHvl after TRPC2 KO (Figure 3, 4, Table 3). While their VMHvl anatomical measures are generally independent of genotype, TRPC2 loss blocks c-fos activation in the VMH of female mice after exposure to a male scent (19). Future examinations of cell characteristics may still identify TRPC2-dependent anatomy in KOs. Additionally, the lateralization that is so pervasive in our measures of the MePD, here and previously (8, 26), is notably absent in the VMH. While the functional significance of laterality is unknown, its role appears minor in the VMHvl and this reassures us that findings of laterality in the MePD are very unlikely to be spurious.

While it is possible the differences between WT and KO mice result from global disruption of brain development, several findings refute this notion. First, many anatomical measures in KO animals match their WT counterparts, including most measures in the female VMHvl. Second, while we found robust genotype differences in regions critically tied to the VNO, none were found in the VMHdm (Figure 3B, 4E, 4F), a region outside the accessory olfactory system (71). This result suggests loss of TRPC2 function in the VNO is the driving factor affecting the KO brain. However, TRPC2 is also expressed in the main olfactory epithelium (72), reproductive organs (73, 74) and, although it is not present in many regions of the adult mouse brain (20), it is expressed by dorsal root and nodose ganglion neurons during development (75). Further research will be necessary to determine where and when TRPC2 expression is important for sexual differentiation of the MePD and VMHvl.

Conclusion

In sum, regional volume and several cellular measures of WT mice show sex and laterality differences in the MePD, while virtually no laterality and few sex differences appear in the VMHvl. TRPC2 KO mice show robust sex- and hemisphere-specific differences from

WT mice. Most of the MePD measures we recorded were affected by TRPC2 KO but the differences varied by sex. Conversely, TRPC2-dependent influence over the VMHvl appears largely limited to males. Thus, the prominent differences in sexual and aggressive behavior between TRPC2 KO mice and controls may be accounted for by the KOs effect on the sexual differentiation of these two brain regions. Future research may examine how and when TRPC2 loss leads to these sex-typical brain changes and how these differences affect behavior in KO mice. In any case, the suggestion that sex differences in the brain may be irrelevant to adult sex differences in behavior, based on findings in TRPC2 KO mice (18), seems to be premature.

Acknowledgments:

The authors would like to thank Kate Mills and Diane Redenius for technical support.

Funding Support:

NSF 12-061, 5R01NS028421-22, 5R01NS045195-16, Michigan State University Graduate School

References

1. Arnold AP, Breedlove SM. Organizational and activational effects of sex steroids on brain and behavior: a reanalysis. Hormones and behavior. 1985;19(4):469–98. [PubMed: 3910535]
2. Yang CF, Chiang MC, Gray DC, Prabhakaran M, Alvarado M, Juntti SA, et al. Sexually dimorphic neurons in the ventromedial hypothalamus govern mating in both sexes and aggression in males. Cell. 2013;153(4):896–909. [PubMed: 23663785]
3. Swift-Gallant A, Niel L, Monks DA. Turning sex inside-out: peripheral contributions to sexual differentiation of the central nervous system. Biology of sex differences. 2012;3(1):12. [PubMed: 22640590]
4. Kiselyov K, van Rossum DB, Patterson RL. TRPC channels in pheromone sensing. Vitam Horm. 2010;83:197–213. [PubMed: 20831947]
5. Alekseyenko O, Baum M, Cherry J. Sex and gonadal steroid modulation of pheromone receptor gene expression in the mouse vomeronasal organ. Neuroscience. 2006;140(4):1349–57. [PubMed: 16626871]
6. Insel TR, Fernald RD. How the brain processes social information: searching for the social brain. Annu Rev Neurosci. 2004;27:697–722. [PubMed: 15217348]
7. Baum MJ. Sexual differentiation of pheromone processing: links to male-typical mating behavior and partner preference. Horm Behav. 2009;55(5):579–88. [PubMed: 19446074]
8. Pfau DR, Hobbs NJ, Breedlove SM, Jordan CL. Sex and laterality differences in medial amygdala neurons and astrocytes of adult mice. Journal of Comparative Neurology. 2016.
9. Dugger BN, Morris JA, Jordan CL, Breedlove SM. Androgen receptors are required for full masculinization of the ventromedial hypothalamus (VMH) in rats. Horm Behav. 2007;51(2):195–201. [PubMed: 17123532]
10. Clancy AN, Coquelin A, Macrides F, Gorski RA, Noble EP. Sexual behavior and aggression in male mice: involvement of the vomeronasal system. J Neurosci. 1984;4(9):2222–9. [PubMed: 6541245]
11. Lee H, Kim D-W, Remedios R, Anthony TE, Chang A, Madisen L, et al. Scalable control of mounting and attack by Esr1+ neurons in the ventromedial hypothalamus. Nature. 2014;509(7502):627–32. [PubMed: 24739975]
12. Leypold BG, Yu CR, Leinders-Zufall T, Kim MM, Zufall F, Axel R. Altered sexual and social behaviors in trp2 mutant mice. Proc Natl Acad Sci U S A. 2002;99(9):6376–81. [PubMed: 11972034]

13. Stowers L, Holy TE, Meister M, Dulac C, Koentges G. Loss of sex discrimination and male-male aggression in mice deficient for TRP2. Science. 2002;295(5559):1493–500. [PubMed: 11823606]
14. Wysocki CJ, Lepri JJ. Consequences of removing the vomeronasal organ. J Steroid Biochem Mol Biol. 1991;39(4B):661–9. [PubMed: 1892795]
15. Pankevich DE, Cherry JA, Baum MJ. Effect of vomeronasal organ removal from male mice on their preference for and neural Fos responses to female urinary odors. Behav Neurosci. 2006;120(4):925–36. [PubMed: 16893298]
16. Bayless DW, Yang T, Mason MM, Susanto AA, Lobdell A, Shah NM. Limbic Neurons Shape Sex Recognition and Social Behavior in Sexually Naive Males. Cell. 2019;176(5):1190–205. e20. [PubMed: 30712868]
17. Martel KL, Baum MJ. Adult testosterone treatment but not surgical disruption of vomeronasal function augments male-typical sexual behavior in female mice. J Neurosci. 2009;29(24):7658–66. [PubMed: 19535577]
18. Kimchi T, Xu J, Dulac C. A functional circuit underlying male sexual behaviour in the female mouse brain. Nature. 2007;448(7157):1009–14. [PubMed: 17676034]
19. Hasen NS, Gammie SC. Trpc2 gene impacts on maternal aggression, accessory olfactory bulb anatomy and brain activity. Genes Brain Behav. 2009;8(7):639–49. [PubMed: 19799641]
20. Zeng C, Tian F, Xiao B. TRPC channels: prominent candidates of underlying mechanism in neuropsychiatric diseases. Molecular neurobiology. 2016;53:631–47. [PubMed: 25502458]
21. Adekunbi D, Li X, Lass G, Shetty K, Adegoke O, Yeo S, et al. Kisspeptin neurones in the posterodorsal medial amygdala modulate sexual partner preference and anxiety in male mice. Journal of neuroendocrinology. 2018;30(3):e12572. [PubMed: 29356147]
22. Aggarwal S, Tang C, Sing K, Kim HW, Millar RP, Tello JA. Medial amygdala Kiss1 neurons mediate female pheromone stimulation of LH in male mice. Neuroendocrinology. 2018.
23. Binns KE, Brennan PA. Changes in electrophysiological activity in the accessory olfactory bulb and medial amygdala associated with mate recognition in mice. Eur J Neurosci. 2005;21(9):2529–37. [PubMed: 15932610]
24. Johnson RT, Schneider A, DonCarlos LL, Breedlove SM, Jordan CL. Astrocytes in the rat medial amygdala are responsive to adult androgens. J Comp Neurol. 2012;520(11):2531–44. [PubMed: 22581688]
25. Johnson RT, Breedlove SM, Jordan CL. Androgen receptors mediate masculinization of astrocytes in the rat posterodorsal medial amygdala during puberty. Journal of Comparative Neurology. 2013;521(10):2298–309. [PubMed: 23239016]
26. Johnson RT, Breedlove SM, Jordan CL. Sex differences and laterality in astrocyte number and complexity in the adult rat medial amygdala. J Comp Neurol. 2008;511(5):599–609. [PubMed: 18853427]
27. Dulce Madeira M, Ferreira-Silva L, Paula-Barbosa MM. Influence of sex and estrus cycle on the sexual dimorphisms of the hypothalamic ventromedial nucleus: stereological evaluation and Golgi study. Journal of Comparative Neurology. 2001;432(3):329–45. [PubMed: 11246211]
28. Chen CV, Brummet JL, Lonstein JS, Jordan CL, Breedlove SM. New knockout model confirms a role for androgen receptors in regulating anxiety-like behaviors and HPA response in mice. Hormones and behavior. 2014;65(3):211–8. [PubMed: 24440052]
29. de Olmos J, Hardy H, Heimer L. The afferent connections of the main and the accessory olfactory bulb formations in the rat: an experimental HRP-study. J Comp Neurol. 1978;181(2):213–44. [PubMed: 690266]
30. Paxinos G, Franklin KB. The mouse brain in stereotaxic coordinates: Gulf Professional Publishing; 2004.
31. Breedlove SM, Cooke BM, Jordan CL. The orthodox view of brain sexual differentiation. Brain, Behavior and Evolution. 1999;54(1):8–14. [PubMed: 10516400]
32. Cooke BM, Breedlove SM, Jordan CL. Both estrogen receptors and androgen receptors contribute to testosterone-induced changes in the morphology of the medial amygdala and sexual arousal in male rats. Hormones and behavior. 2003;43(2):336–46. [PubMed: 12694644]

33. Morris JA, Jordan CL, King ZA, Northcutt KV, Breedlove SM. Sexual dimorphism and steroid responsiveness of the posterodorsal medial amygdala in adult mice. Brain Res. 2008;1190:115–21. [PubMed: 18054901]
34. McGregor A, Herbert J. Differential effects of excitotoxic basolateral and corticomedial lesions of the amygdala on the behavioural and endocrine responses to either sexual or aggression-promoting stimuli in the male rat. Brain research. 1992;574(1–2):9–20. [PubMed: 1386276]
35. Maras PM, Petrulis A. Lesions that functionally disconnect the anterior and posterodorsal subregions of the medial amygdala eliminate opposite-sex odor preference in male Syrian hamsters (Mesocricetus auratus). Neuroscience. 2010;165(4):1052–62. [PubMed: 19931356]
36. Coolen LM, Wood RI. Bidirectional connections of the medial amygdaloid nucleus in the Syrian hamster brain: simultaneous anterograde and retrograde tract tracing. Journal of Comparative Neurology. 1998;399(2):189–209. [PubMed: 9721903]
37. Olds JL, Bhalla US, McPhie DL, Lester DS, Bower JM, Alkon DL. Lateralization of membrane-associated protein kinase C in rat piriform cortex: specific to operant training cues in the olfactory modality. Behavioural brain research. 1994;61(1):37–46. [PubMed: 8031495]
38. Cohen Y, Putrino D, Wilson DA. Dynamic cortical lateralization during olfactory discrimination learning. The Journal of physiology. 2015;593(7):1701–14. [PubMed: 25604039]
39. Kucharski D, Johanson IB, Hall W. Unilateral olfactory conditioning in 6-day-old rat pups. Behavioral and neural biology. 1986;46(3):472–90. [PubMed: 3814049]
40. Jozet-Alves C, Percelay S, Bouet V. Olfactory Laterality Is Valence-Dependent in Mice. Symmetry. 2019;11(9):1129.
41. Siniscalchi M, Sasso R, Pepe AM, Dimatteo S, Vallortigara G, Quaranta A. Sniffing with the right nostril: lateralization of response to odour stimuli by dogs. Animal behaviour. 2011;82(2):399–404.
42. Moncho-Bogani J, Martinez-Garcia F, Novejarque A, Lanuza E. Attraction to sexual pheromones and associated odorants in female mice involves activation of the reward system and basolateral amygdala. European Journal of Neuroscience. 2005;21(8):2186–98. [PubMed: 15869515]
43. Roberts SA, Simpson DM, Armstrong SD, Davidson AJ, Robertson DH, McLean L, et al. Darcin: a male pheromone that stimulates female memory and sexual attraction to an individual male's odour. BMC biology. 2010;8(1):75. [PubMed: 20525243]
44. Hasen NS, Gammie SC. Trpc2-deficient lactating mice exhibit altered brain and behavioral responses to bedding stimuli. Behav Brain Res. 2011;217(2):347–53. [PubMed: 21070815]
45. Zatorre RJ, Jones-Gotman M. Right-nostril advantage for discrimination of odors. Percept Psychophys. 1990;47(6):526–31. [PubMed: 2367173]
46. Savic I, Berglund H. Right-nostril dominance in discrimination of unfamiliar, but not familiar, odours. Chem Senses. 2000;25(5):517–23. [PubMed: 11015323]
47. Kelliher KR, Spehr M, Li XH, Zufall F, Leinders-Zufall T. Pheromonal recognition memory induced by TRPC2-independent vomeronasal sensing. European Journal of Neuroscience. 2006;23(12):3385–90. [PubMed: 16820028]
48. Bellringer JF, Pratt HP, Keverne EB. Involvement of the vomeronasal organ and prolactin in pheromonal induction of delayed implantation in mice. J Reprod Fertil. 1980;59(1):223–8. [PubMed: 7401039]
49. Lonstein JS, Simmons DA, Stern JM. Functions of the caudal periaqueductal gray in lactating rats: kyphosis, lordosis, maternal aggression, and fearfulness. Behav Neurosci. 1998;112(6):1502–18. [PubMed: 9926832]
50. Wersinger S, Rissman E. Oestrogen receptor α is essential for female-directed chemo-investigatory behaviour but is not required for the pheromone-induced luteinizing hormone surge in male mice. Journal of neuroendocrinology. 2000;12(2):103–10. [PubMed: 10718905]
51. Lo L, Yao S, Kim D-W, Cetin A, Harris J, Zeng H, et al. Connectional architecture of a mouse hypothalamic circuit node controlling social behavior. Proceedings of the National Academy of Sciences. 2019;116(15):7503–12.
52. Lonstein JS, Stern JM. Role of the midbrain periaqueductal gray in maternal nurturance and aggression: c-fos and electrolytic lesion studies in lactating rats. J Neurosci. 1997;17(9):3364–78. [PubMed: 9113892]

53. Ishii KK, Osakada T, Mori H, Miyasaka N, Yoshihara Y, Miyamichi K, et al. A labeled-line neural circuit for pheromone-mediated sexual behaviors in mice. Neuron. 2017;95(1):123–37. e8. [PubMed: 28648498]
54. Wersinger SR, Baum MJ. Sexually dimorphic processing of somatosensory and chemosensory inputs to forebrain luteinizing hormone-releasing hormone neurons in mated ferrets. Endocrinology. 1997;138(3):1121–9. [PubMed: 9048618]
55. Pardo-Bellver C, Cádiz-Moretti B, Novejarque A, Martínez-García F, Lanuza E. Differential efferent projections of the anterior, posteroventral, and posterodorsal subdivisions of the medial amygdala in mice. Frontiers in neuroanatomy. 2012;6:33. [PubMed: 22933993]
56. Ivanova D, Li X-F, McIntyre C, O'Byrne KT. Posterodorsal medial amygdala urocortin-3, GABA and glutamate mediate suppression of LH pulsatility in female mice. bioRxiv. 2022:2022.07.07.499104.
57. Allen NJ, Barres BA. Neuroscience: glia—more than just brain glue. Nature. 2009;457(7230):675. [PubMed: 19194443]
58. Chowen JA, Garcia-Segura LM. Role of glial cells in the generation of sex differences in neurodegenerative diseases and brain aging. Mechanisms of Ageing and Development. 2021;196:111473.
59. McCARTHY MM TODD BJ, AMATEAU SK. Estradiol modulation of astrocytes and the establishment of sex differences in the brain. Annals of the New York Academy of Sciences. 2003;1007(1):283–97. [PubMed: 14993061]
60. Lenz KM, McCarthy MM. A starring role for microglia in brain sex differences. The Neuroscientist. 2015;21(3):306–21. [PubMed: 24871624]
61. VanRyzin J Microglia Regulation of Sexually Dimorphic Amygdala Development 2019.
62. Nordeen EJ, Nordeen KW. Sex difference among nonneuronal cells precedes sexually dimorphic neuron growth and survival in an avian song control nucleus. J Neurobiol. 1996;30(4):531–42. [PubMed: 8844516]
63. Matsumoto A, Arai Y. Sex difference in volume of the ventromedial nucleus of the hypothalamus in the rat. Endocrinologia japonica. 1983;30(3):277–80. [PubMed: 6662066]
64. Rasia-Filho A, Fabian C, Rigoti K, Achaval M. Influence of sex, estrous cycle and motherhood on dendritic spine density in the rat medial amygdala revealed by the Golgi method. Neuroscience. 2004;126(4):839–47. [PubMed: 15207319]
65. Larriva-Sahd J, Rondan-Zarate A, Ramirez-Degollado M. Sexually dimorphic contribution from the fornix to the ventromedial hypothalamic nucleus: a quantitative electron microscopic study. Neurosci Lett. 1995;200(3):147–50. [PubMed: 9064598]
66. McQueen JK, Wright AK, Arbuthnott GW, Fink G. Glial fibrillary acidic protein (GFAP)immunoreactive astrocytes are increased in the hypothalamus of androgen-insensitive testicular feminized (Tfm) mice. Neuroscience letters. 1990;118(1):77–81. [PubMed: 1701870]
67. Lin D, Boyle MP, Dollar P, Lee H, Lein E, Perona P, et al. Functional identification of an aggression locus in the mouse hypothalamus. Nature. 2011;470(7333):221–6. [PubMed: 21307935]
68. Sano K, Tsuda MC, Musatov S, Sakamoto T, Ogawa S. Differential effects of site-specific knockdown of estrogen receptor α in the medial amygdala, medial pre-optic area, and ventromedial nucleus of the hypothalamus on sexual and aggressive behavior of male mice. European Journal of Neuroscience. 2013;37(8):1308–19. [PubMed: 23347260]
69. Araque A, Parpura V, Sanzgiri RP, Haydon PG. Tripartite synapses: glia, the unacknowledged partner. Trends in neurosciences. 1999;22(5):208–15. [PubMed: 10322493]
70. Gordon GR, Iremonger KJ, Kantevari S, Ellis-Davies GC, MacVicar BA, Bains JS. Astrocytemediated distributed plasticity at hypothalamic glutamate synapses. Neuron. 2009;64(3):391–403. [PubMed: 19914187]
71. Keverne EB. The vomeronasal organ. Science. 1999;286(5440):716–20. [PubMed: 10531049]
72. Omura M, Mombaerts P. Trpc2-expressing sensory neurons in the main olfactory epithelium of the mouse. Cell Rep. 2014;8(2):583–95. [PubMed: 25001287]
73. Jungnickel MK, Marrero H, Birnbaumer L, Lémos JR, Florman HM. Trp2 regulates entry of Ca2+ into mouse sperm triggered by egg ZP3. Nature Cell Biology. 2001;3(5):499. [PubMed: 11331878]

74. De Clercq K, Van den Eynde C, Hennes A, Van Bree R, Voets T, Vriens J. The functional expression of transient receptor potential channels in the mouse endometrium. Human Reproduction. 2017;32(3):615–30. [PubMed: 28077439]

75. Elg S, Marmigere F, Mattsson JP, Ernfors P. Cellular subtype distribution and developmental regulation of TRPC channel members in the mouse dorsal root ganglion. Journal of Comparative Neurology. 2007;503(1):35–46. [PubMed: 17480026]

Key Points:

1. TRPC2 is critical to the appearance of anatomical sex differences in adult mouse MePD and VMHvl
2. *TRPC2* loss alters MePD anatomy in both males and females
3. *TRPC2* loss alters the VMHvl of males but has little influence over VMHvl anatomy in females

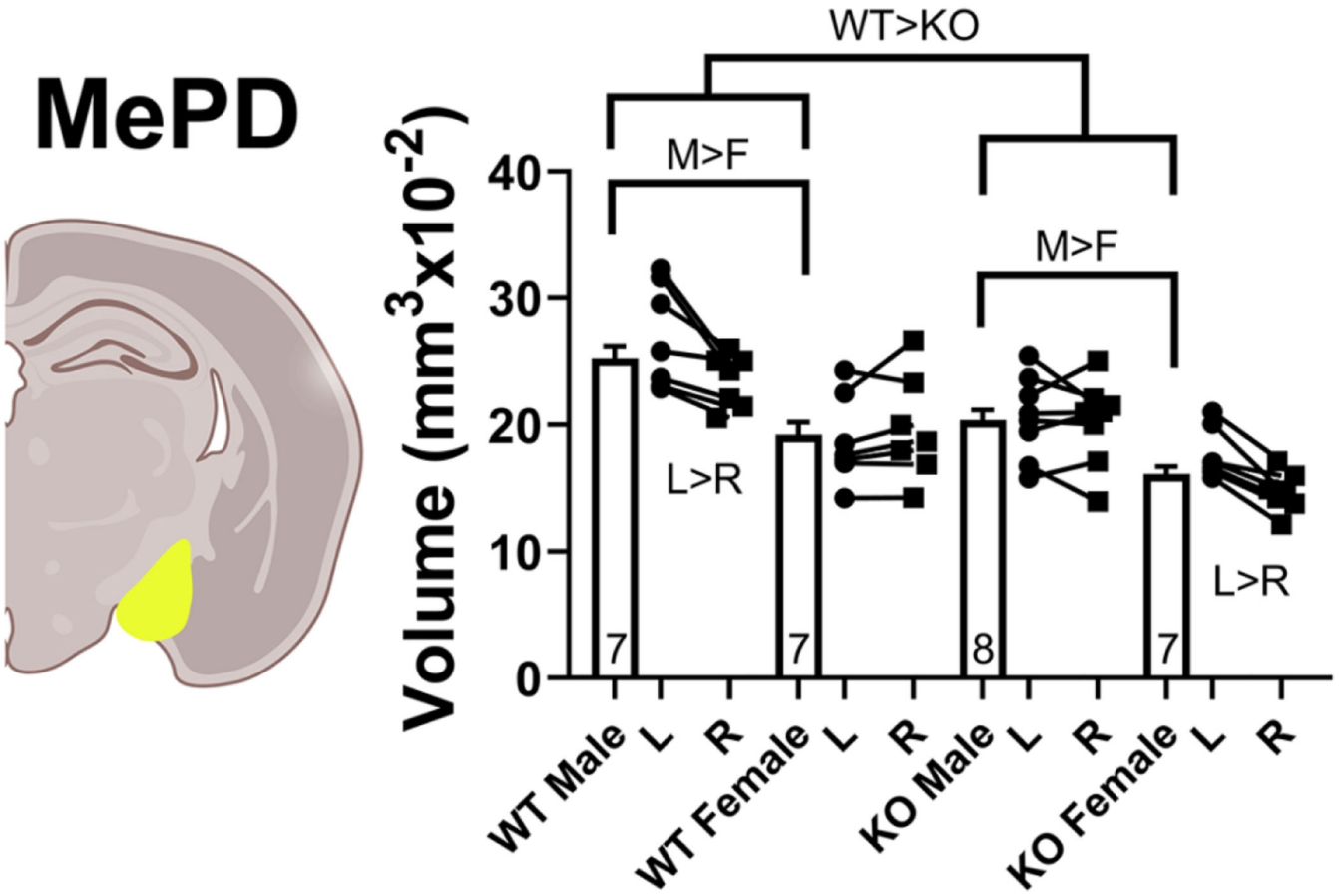

Figure 1: Loss of TRPC2 signaling alters posterodorsal aspect of the medial amygdala (MePD) regional volume in a sex- and hemisphere-specific manner.

(i) WT adult B6/129S males (M) have larger MePD than females (F) and the MePD of WT males is also lateralized, being larger in the right (R) hemisphere than the left (L) in Nissl-stained sections. MePD volume is not lateralized in WT females. In TRPC2 KO mice, the sex difference remains in the right hemisphere but is lost in the left. TRPC2 loss reduced MePD volume in both sexes, in a lateralized manner, significantly decreasing the left MePD in KO males, and significantly decreasing the right MePD in KO females. Consequently, the lateralization of MePD is lost in KO males, while the KO induces laterality in females that is absent in WT females. These complex effects of TRPC2 loss on the MePD suggest sex-specific and lateralized mechanisms regulate the sex-specific behaviors altered in KOs. Bar values are group means ± standard errors of the mean; numbers on bars indicate the n per group. Data points are individual values by hemisphere. The symbols > and < indicate significant main effects of sex or genotype and within-subject laterality with $p<0.05$.

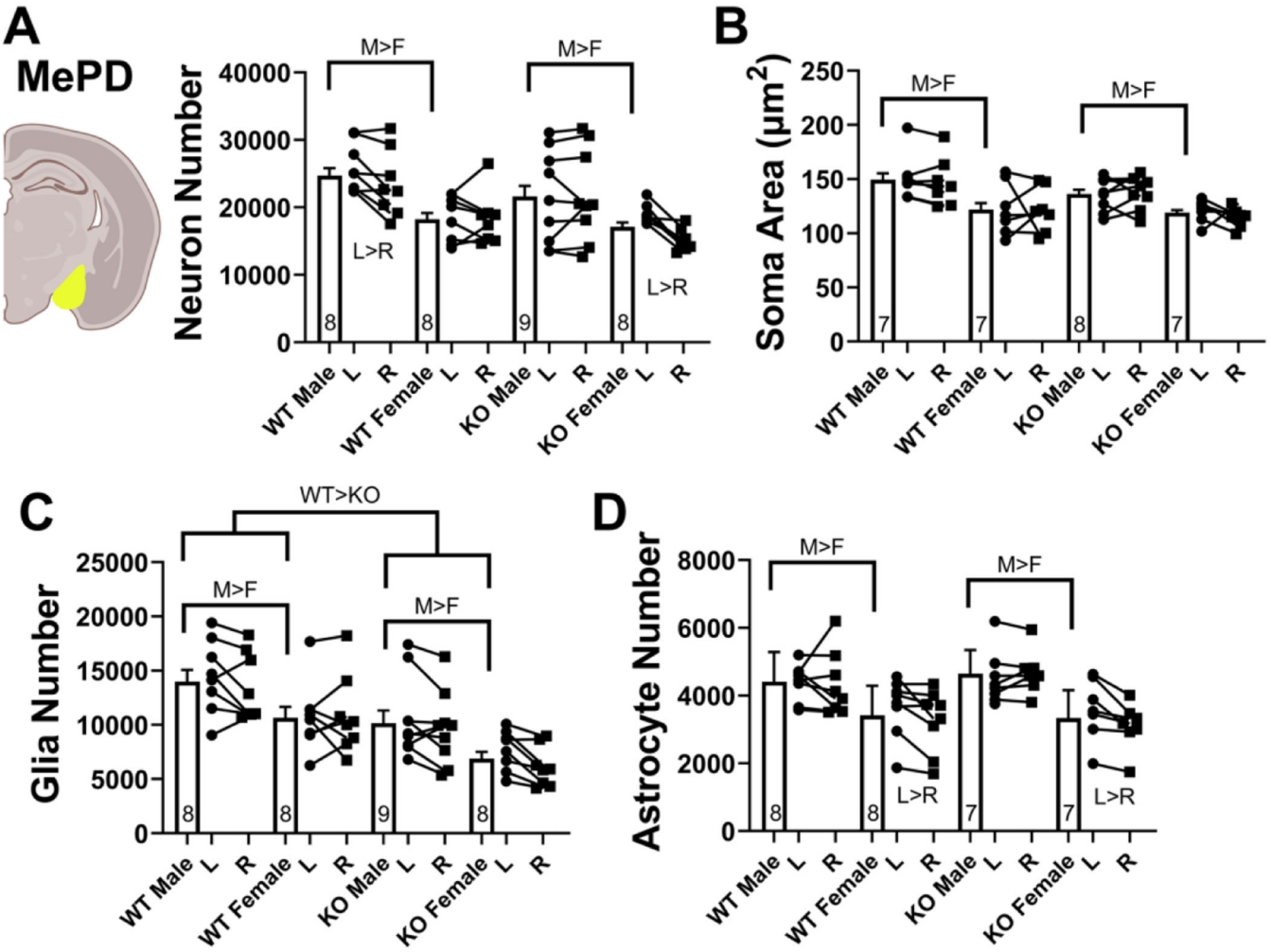

Figure 2: Sex differences and laterality of the adult posterodorsal aspect of the medial amygdala (MePD) are affected in TRPC2 KO mice.

A MePD in Nissl-stained sections from males (M) have more neurons than females (F), regardless of genotype. There was no significant effect of genotype on this measure ($F_{(1,29)}$=3.16, p=0.086). A(ii) Looking across hemispheres, the sex difference in the lateralized number of MePD neurons in WT mice is flipped by the loss in TRPC2, where only females display laterality. In short, the number of neurons shows sex differences in the left (L) hemisphere of WT mice, while KO mice show sex differences in number of neurons only on the right (R). B Neuronal somata are larger in male mice than females, regardless of genotype or hemisphere. C The number of glia in the MePD is greater in males than females, in both WT and KO mice, and is also reduced in KO mice compared to WTs. This count includes all glia types i.e., it does not differentiate between astrocytes, microglia, oligodendrocytes etc. While TRPC2 loss significantly reduced glial number the sex difference is retained, KO males have more glia than KO females. There were no hemisphere differences in overall glial number in Nissl-stained sections from either genotype in Nissl stain. D In glial fibrillary acidic protein-(GFAP)-stained tissue, the MePD males have more astrocytes than females in both WT and KO mice, and there was no main effect of genotype on this measure. In both WT and KO mice, females have more astrocytes

in the left MePD than the right. These data show that TRPC2 has a significant influence in determining many cellular attributes of the adult MePD that may contribute to behavioral effects in KO mice. Bar values are group means ± standard errors of the mean, numbers on bars indicate the n per group. Data points are individual values by hemisphere. The symbols > and < indicate main effects of sex or genotype and within-subject laterality with $p<0.05$.

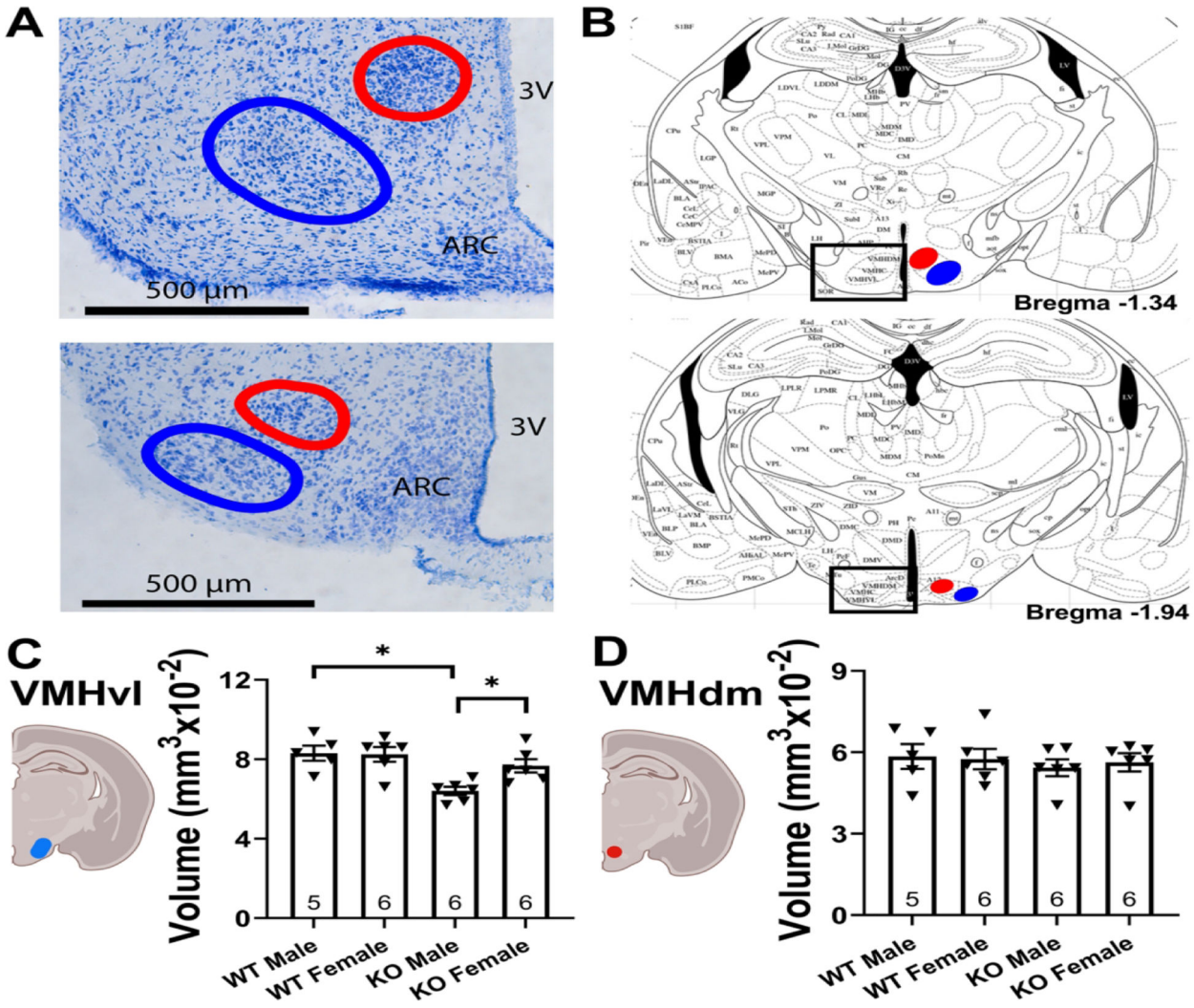

Figure 3: Loss of TRPC2 introduces a sex difference in the regional volume of the ventromedial hypothalamus (VMH).

A) The volume of the ventrolateral (vl) subdivision of the VMH was reduced in TRPC2 KO mice, but only in males. B) Volume of the dorsomedial (dm) subdivision of the VMH was not affected by sex or genotype. There was no laterality detected in any measures of the VMH, in either genotype. Bar values are means ± standard error of the mean, data points are individual values averaged across hemisphere, bar numbers indicate the n per group, *=significant gene by sex interactions with $p<0.05$.

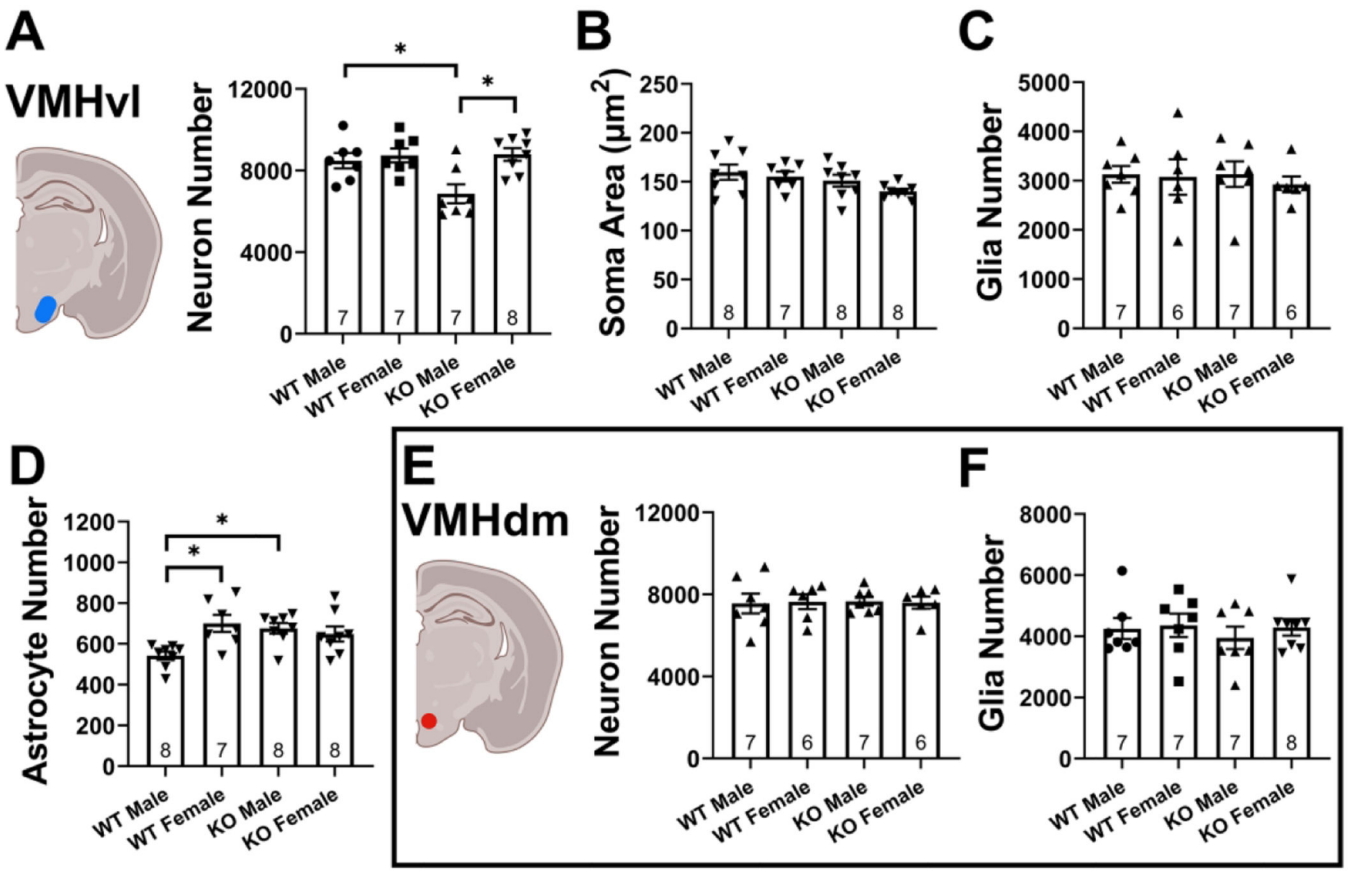

Figure 4: TRPC2 KO affects neuronal size in the ventromedial hypothalamus (VMH).

A) There was no sex difference in the number of neurons in the VMH ventrolateral subdivision (vl) of WT mice, but TRPC2 KO reduced the number of neurons in males only. B) TRPC2 KO reduced the size of VMHvl neurons in both sexes. C) The number of overall glia in the VMHvl displayed neither a sex difference nor an effect of genotype in Nissl stained sections. D) The number of astrocytes seen in glial fibrillary acidic protein-stained sections was lower in males than in females for WT mice, but this sex difference was lost in TRPC2 KO mice due to an increase in astrocyte number in KO males. E, F) In contrast to measures of the vl subdivision of the VMH, there were no effects of sex or genotype on neither neuronal number nor number of glia in the dorsomedial (dm) subdivision. Bar values are means ± standard error of the mean, data points are individual values averaged across hemispheres, bar number represents n per group, *=significant gene by sex interactions with $p<0.05$.

Table 1:

List of Antibodies Used for GFAP Immunohistochemistry

Antigen	Description of Immunogen	Source, Host Species, Cat. #, Clone or Lot#, RRID	Concentration Used
Glial Fibrillary Acidic Protein clone GA5	Purified porcine spinal cord Glial Fibrillary Acidic Protein	EMD Millipore, mouse monoclonal, Cat# MAB360, RRID:AB_2109815	0.02 μl/ml
Anti-mouse IgG	Mouse IgG (H+L), rat absorbed, biotinylated	Vector Laboratories, horse polyclonal, Cat# BA-2001, RRID:AB_2336180	0.4 μl/ml

Table 2:

Statistical measures of MePD astrocyte complexity (bolded numbers are significantly greater; Mean±SEM).

	FEMALES		MALES		Sex		Genotype		Laterality	
	TRPC2 +/+	TRPC2 −/−	TRPC2 +/+	TRPC2 −/−	$F_{(1,16)}$	P	$F_{(1,16)}$	P	$F_{(1,16)}$	P
Branch number	5.47 ± 0.14	5.01 ± 0.21	5.47 ± 0.17	5.37 ± 0.13	1.22	0.29	1.17	0.3	1.38	0.26
Node Number	16.31 ± 1.31	14.42 ± 0.8	14.85 ± 1.2	12.89 ± 0.59	2.11	0.17	3.48	0.08	1.83	0.19
End Number	**22.18 ± 1.27**	19.5 ± 0.95	**20.2 ± 1.05**	18.58 ± 0.71	2.04	0.172	**4.48**	**0.05**	2.4	0.14
Total Length	291.9 ± 12.9	257.6 ± 20.2	260.7 ± 12.9	252.1 ± 13.2	1.79	0.2	2.43	0.14	1.53	0.24
Mean Branch Length	53.03 ± 3.86	52.95 ± 2.96	48.93 ± 1.37	46.43 ± 1.31	4.14	0.06	0.245	0.63	0.058	0.81

Table 3:

Statistical measures of VMHvl astrocyte complexity (bolded numbers are significantly greater based on main effects and interactions; Mean±SEM).

	FEMALES		MALES		Sex		Gene		Laterality	
	TRPC2 +/+	**TRPC2 −/−**	**TRPC2 +/+**	**TRPC2 −/−**	$F_{(1,17)}$	***P***	$F_{(1,17)}$	***P***	$F_{(1,17)}$	***P***
Branch number	5.1 ± 0.22	5.15 ± 0.18	5.22 ± 0.23	5.0 ± 0.21	0.002	0.97	0.14	0.71	0.01	0.98
Node Number	**20.2 ± 0.54**	**19.43 ± 0.96**	**21.15 ± 0.9**	15.8 ± 1.45	1.54	0.23	**8**	**0.012**	0.58	0.46
End Number	**26.32 ± 1.52**	**27.31 ± 1.92**	**25.99 ± 1.44**	20.51 ± 1.13	**5.68**	**0.029**	2.25	0.15	0.013	0.91
Total Length	329.15 ± 43.5	305.21 ± 25.4	333.86 ± 13.5	275.26 ± 23.4	0.2	0.66	2.13	0.16	1.39	0.25
Mean Branch Length	64.51 ± 8.09	59.66 ± 4.01	65.19 ± 5.23	55.29 ± 4.14	0.113	0.74	1.8	0.2	0.78	0.39